Influence of Tempering Temperature on Stability of Carbide Phases in 2.6Cr-0.7Mo-0.3V Steel with Various Carbon Content

J. JANOVEC, A. VYROSTKOVA, and M. SVOBODA

The present work evaluates the influence of the bulk carbon content (0.1, 0.006, and 0.005 wt pct) and tempering temperature (823, 853, and 913 K) on stability, chemical composition, and size of carbide particles in 540 ks tempered states of 2.6Cr-0.7Mo-0.3V steel. The scanning transmission electron microscopy/energy-dispersive X-ray spectroscopy (STEM/EDXS) and electron diffraction methods were used to analyze the carbide particles. A characteristic energy-dispersive X-ray (EDX) spectrum can be attributed to each of the identified carbides. The MC carbide is stable in all experimental states. The phase stability of Fe-Cr-rich carbides increased in the order ε, $Fe_3C \rightarrow M_3C \rightarrow M_7C_3$, with tempering temperature increasing. In steels with higher carbon content tempered at low temperature, $M_{23}C_6$ carbide was also noted. The Mo_2C and M_6C carbides were not observed. It was shown that the decrease of the bulk carbon content has the same influence on the carbide phases stability as the increase of the bulk vanadium content at the unchanged Cr, Mo, C bulk contents and tempering temperature. Similarly, the decrease of tempering temperature has the same influence on the carbide phases stability as the decrease of the bulk Cr content at the unchanged V, Mo, and C bulk contents.

I. INTRODUCTION

AUSTENITIZATION, quenching, and tempering are procedures often used in the heat treatment of the low-alloy steels. The transition from the quenched to the tempered state is usually accompanied by precipitation of metastable carbides, by changes in crystal structure,[1,2] chemical composition,[3,4] and size[5] of carbide particles, and by recovery of the ferrite. The character, mechanism, and kinetics of these changes depend on three main factors:

(a) the chemical composition of the steel;[3,6]
(b) the microstructure and phase composition of the quenched state;[7] and
(c) the tempering temperature.[8,9]

The chemical composition of the steel, tempering time (t_T), and tempering temperature (T_T) also directly affect the phase constitution of long-term tempered state. This is evident from Table I, containing the data by Kuo,[1] Andrews *et al.*,[6] Čadek *et al.*,[10] and Shaw and Quarrell.[12] Smith[11] and Quarrell[12,13] formed carbide phases constitution diagrams to summarize their results. An example of such a diagram for 0.2C-0.5Mo-yCr-zV (wt. pct) steel at 973 K is given in Figure 1,[11] where y and z specify the bulk content of Cr and V, respectively.

The chemical composition of the steel, tempering temperature, and time also influence the chemical composition of the carbide metallic constituent (M).[3,14] This is strongly evident for the M_3C and MC carbides.[15] Energy-dispersive X-ray (EDX) analyses taken using scanning transmission electron microscopy (STEM) revealed that each carbide has a characteristic EDX spectrum,[3,4,16,17] as shown in Figure 2 for Cr-Mo steels.[18]

The aim of the present work is to determine the influence of the bulk carbon content and tempering temperature on the phases stability, chemical compositions, and sizes of carbide particles in 540 ks tempered states of 2.6Cr-0.7Mo-0.3V-based steels.

II. METHODS

Three casts (A, B, C) of low-alloy 2.6Cr-0.7Mo-0.3V steel with different carbon contents (Table II) were prepared by melting in a vacuum-induction furnace. Cylindrical ingots weighing 2 kg were forged to bars of 15 × 15-mm square section. Samples, 15 × 15 × 25 mm, were placed into evacuated quartz capsules and heat-treated according to the schedules given in Table III.

The average austenite grain size (d_γ) and microstructures of the experimental states were characterized by means of light microscopy (LM).

Thin foils and carbon extraction replicas were examined in a PHILIPS* CM12 STEM operating at 120 kV with energy-dispersive X-ray microanalyzer EDAX 9900 to determine the crystal structure of the extracted carbides, the metallic elements contents of the carbides, and the average sizes (d) of carbide particles. The X-ray spectra were acquired in STEM mode, with count rates from 100 to 200 cps obtained using a spot size appropriate for the size of the analyzed carbide. Semiquantitative analyses of the EDX spectra were carried out according to the EDAX standardless method for thin samples. No corrections for absorption or fluorescence

*PHILIPS is a trademark of Philips Electronic Instruments Corp., Mahwah, NJ.

J. JANOVEC, Research Staff Member, and A. VYROSTKOVA, Research Worker, are with Slovak Academy of Sciences, Institute of Materials Research, 043 53-Kosice, Watsonova 47, Slovakia. M. SVOBODA, Research Staff Member, is with Academy of Sciences of the Czech Republic, Institute of Physical Metallurgy, 616 62-Brno, Zizkova 22, Czech Republic.

Manuscript submitted December 21, 1992.

Table I. Influence of Bulk Chemical Composition and Tempering Conditions on the Composition of Equilibrium Carbides

Reference	Steel Composition (Wt Pct) C	Cr	Mo	V	T_T (K)	t_T (ks)	Phase Composition Equilibrium Carbides
1	0.18	—	3.88	—	973	18,000	M_6C + MoC
	0.23	—	6.10	—	973	18,000	M_6C
	0.23	—	0.80	—	973	18,000	M_3C + MoC
10	0.37	1.35	0.48	—	923	18,000	M_2C + M_7C_3
	0.47	4.51	0.56	—	923	18,000	M_7C_3
	0.42	4.22	1.15	—	923	18,000	M_7C_3 + $M_{23}C_6$ + M_6C
	0.36	4.74	2.13	—	923	18,000	$M_{23}C_6$ + M_6C
6	0.12	0.50	0.80	0.50	923	3,600	MC
	0.12	2.60	0.80	0.50	923	3,600	MC + M_7C_3 + M_6C
	0.12	5.20	0.80	0.50	923	3,600	MC + $M_{23}C_6$ + M_6C
	0.12	0.50	0.80	0.50	973	3,600	MC + M_2C
	0.12	2.60	0.80	0.50	973	3,600	MC + M_7C_3 + M_6C
	0.12	5.20	0.80	0.50	973	3,600	MC + $M_{23}C_6$
12	0.21	—	—	0.34	973	3,600	MC + Fe_3C
	0.23	2.02	—	0.21	973	3,600	MC + M_7C_3
	0.21	8.91	—	0.38	973	3,600	$M_{23}C_6$

were made, because the average size of the carbides was below 250 nm.

III. RESULTS

Ferrite and carbide particles, as products of the decomposition of martensite and bainite, are present in the microstructure of the tempered state A3, with both the highest carbon content and the highest tempering temperature. Similar microstructure is also seen in A1 and A2 states, which are tempered at lower temperatures, and in all states of the cast B, with lower carbon content. Fewer carbide particles in initially bainitic and acicular ferrite areas were observed in the microstructure of the tempered states of the cast C, with the lowest carbon content. Because of the similarity of A1 through A3, B1 through B3, and C1 through C3 states, only the states

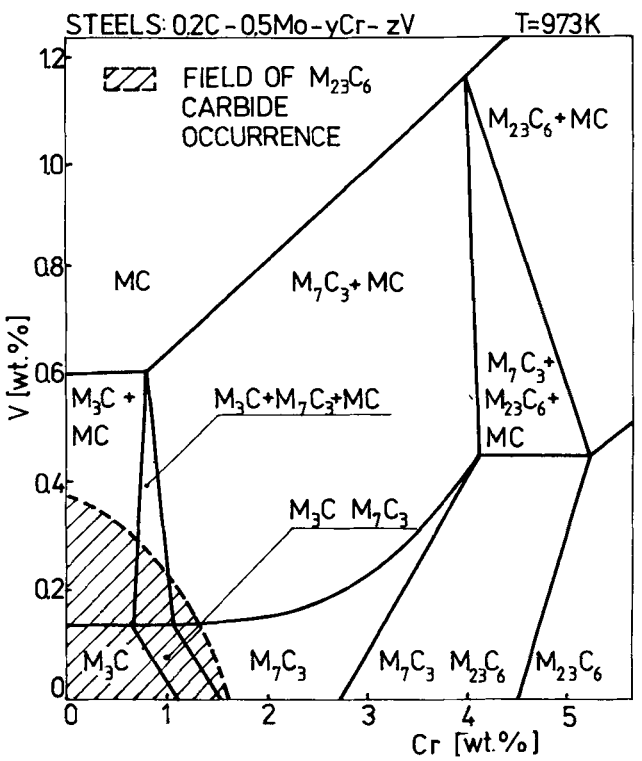

Fig. 1—Constitution diagram of carbide phases in 0.2C-0.5Mo-yCr-zV steels at the temperature 973 K.[111]

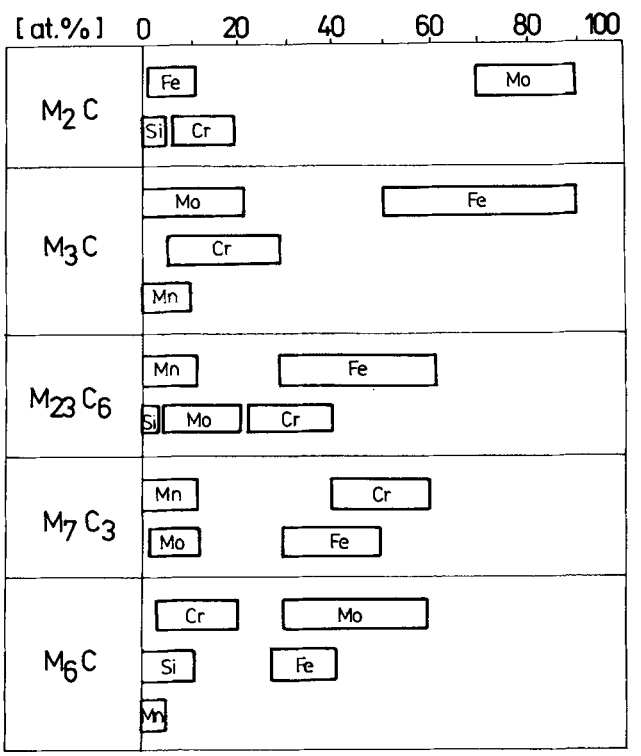

Fig. 2—Chemical composition of metallic constituent of carbides in Cr-Mo steels.[118]

Table II. Chemical Composition of Experimental Steels (in Weight Percent)

Steel	C	Mn	Si	Cr	Mo	V	P	S
A	0.100	0.70	0.27	2.62	0.69	0.33	0.014	0.006
B	0.060	0.65	0.29	2.66	0.70	0.31	0.013	0.006
C	0.005	0.64	0.24	2.63	0.69	0.34	0.017	0.006

Table III. Heat Treatment of Experimental Steels

Heat Treatment	States
Austenitized 1513 K/0.6 ks, water quenched	A0, B0, C0
Austenitized 1513 K/0.6 ks, water quenched, tempered 823 K/540 ks, cooled 300 K/s	A1, B1, C1
Austenitized 1513 K/0.6 ks, water quenched, tempered 853 K/540 ks, cooled 300 K/s	A2, B2, C2
Austenitized 1513 K/0.6 ks, water quenched, tempered 913 K/540 ks, cooled 300 K/s	A3, B3, C3

Table IV. Average Size of Prior Austenite Grains (d_γ) and Occurrence of Carbide Phases in the Experimental States

State	d_γ (mm)	Carbide Phases
A0	0.30	ε, Fe_3C
A1	0.30	M_7C_3, M_3C, $M_{23}C_6$, MC
A2	0.30	M_7C_3, $M_{23}C_6$, MC
A3	0.30	M_7C_3, MC
B0	0.30	ε, Fe_3C
B1	0.30	M_7C_3, M_3C, $M_{23}C_6$, MC
B2	0.30	M_7C_3, MC
B3	0.30	M_7C_3, MC
C0	0.22	Fe_3C
C1	0.22	MC
C2	0.22	MC
C3	0.22	MC

tempered at the highest temperature are documented in Figures 3(a) through (c). The prior austenite grains of the quenched states, A0, B0, and C0, can be seen in the upper right-hand corners of Figures 3(a) through (c), and their average sizes are given in Table IV.

Transmission electron microscopy (TEM) observations of the quenched states (thin foils) showed that the states A0 (Figure 4(a)) and B0 (Figure 4(b)) have martensitic-bainitic microstructure containing retained austenite and ε and Fe_3C carbides. The plate-shaped particles of ε-carbide appear in the inner part of self-tempered martensitic laths. Between bainitic laths, the particles of Fe_3C were observed. Upper bainite and acicular ferrite (Figure 4(c)) form the microstructure of the state C0. The presence of Fe_3C carbide particles in this state is rare; MC particles were not observed (Table IV). All tempered states exhibited ferritic-carbidic microstructure, and four carbide types were identified: M_3C, $M_{23}C_6$, M_7C_3, and MC. Characteristic EDX spectra of the carbides are given in Figures 5(a) through (d). The majority of the Fe-Cr-rich carbide particles occurring in the microstructures of states A1, A2, and B1 are of the M_7C_3 type. The presence of $M_{23}C_6$ carbide particles in these states is rare; M_3C particles were observed only in the states A1 and B1. Carbide phases present in the tempered states, as a function of tempering temperature and bulk carbon content, are given in Table IV and plotted in the form of a constitution diagram in Figure 6. According to localization of experimental points, the boundaries of four carbide phase stability areas, M_3C + $M_{23}C_6$ + M_7C_3 + MC, $M_{23}C_6$ + M_7C_3 + MC, M_7C_3 + MC, and MC, were established. These are labeled by dashed lines in Figure 6.

Carbide particles morphology and distribution in the tempered steels are shown in Figure 7. As the tempering temperature increased, the number of particles per unit area decreased, and their size increased. The influence of tempering temperature and bulk carbon content on the average size of various carbide-type particles is given in Figure 8. The largest dimension of the particles was used to evaluate their average size, according to the method of Purmensky *et al.*[5] It can be seen that the largest particles are M_7C_3 carbides, and that MC are the smallest ones. The average size of the M_3C and $M_{23}C_6$ particles is comparable.

About 300 particles were analyzed by STEM/EDXS, with the carbide structures being verified by selected-area electron diffraction. These results are summarized in Table V. In the metallic constituent of M_3C, $M_{23}C_6$, and M_7C_3 carbides, the elements Mo, V, Cr, Mn, and Fe were identified. Fe and Cr were the dominant elements. Only V and Mo were found in the metallic constituent of MC carbide. Table V shows the changes in the chemical compositions of carbides M_3C, $M_{23}C_6$, M_7C_3, and MC as a function of T_T and bulk carbon content.

IV. DISCUSSION

A. *Stability of Carbide Phases*

From the phase stability point of view, the carbides identified in the tempered steels can be characterized as follows (Figure 6):

1. MC is the most stable carbide. Its stability is not influenced by the bulk carbon content and tempering temperature.
2. $M_{23}C_6$, usually the most stable among Cr-rich carbides,[18] in the experimental steel was found only in the states A1, A2, and B1, which had higher bulk carbon contents tempered at lower temperatures.

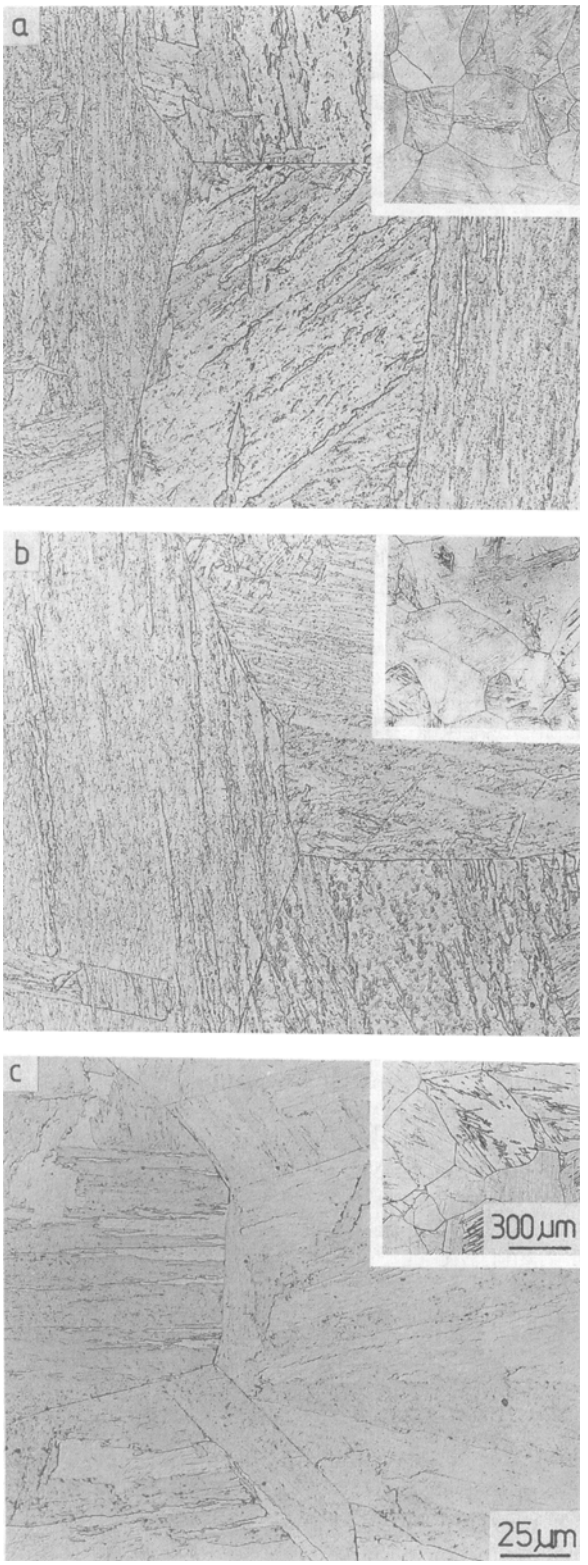

Fig. 3 — Microstructures of the tempered states and prior austenite grains of quenched states (upper right-hand corner), LM: (*a*) A3, A0; (*b*) B3, B0; and (*c*) C3, C0.

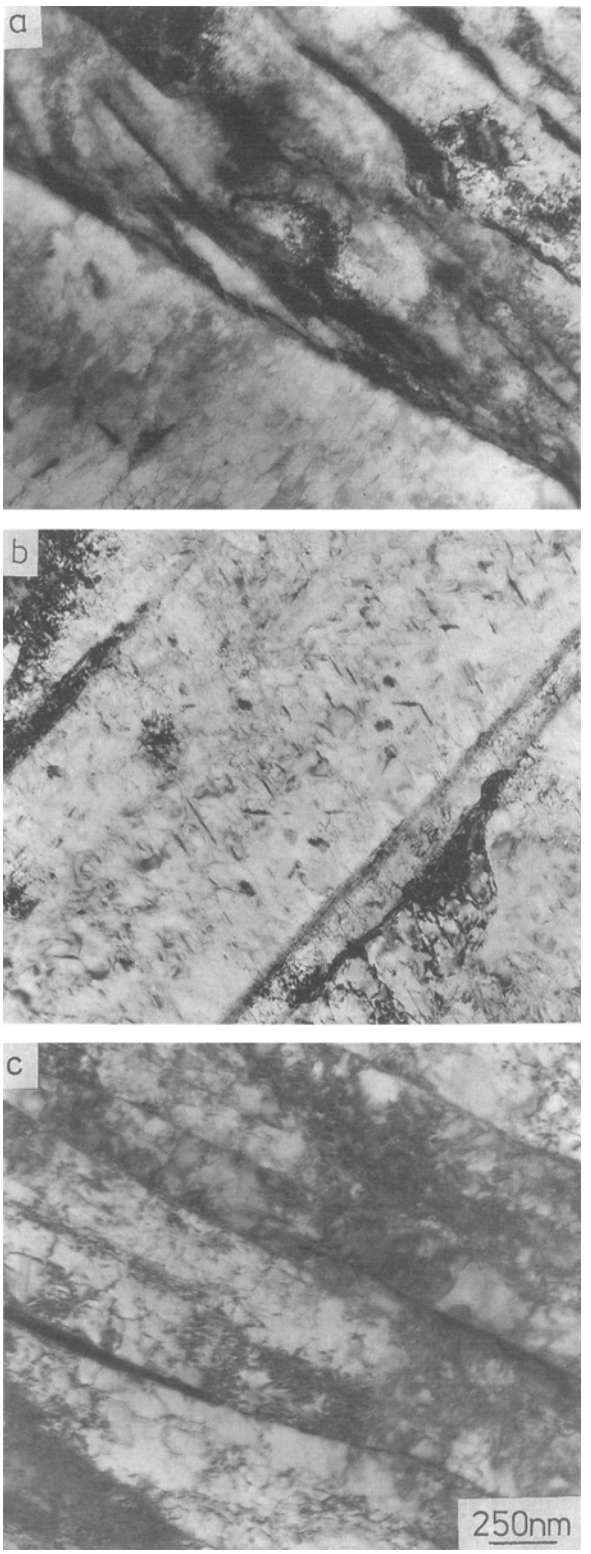

Fig. 4 — Substructure of the quenched states, TEM, thin foils: (*a*) martensite and retained austenite (interlath dark areas) in state A0; (*b*) particles of $\varepsilon-$ and M_3C carbides in self-tempered martensite, state B0; and (*c*) acicular ferrite in state C0.

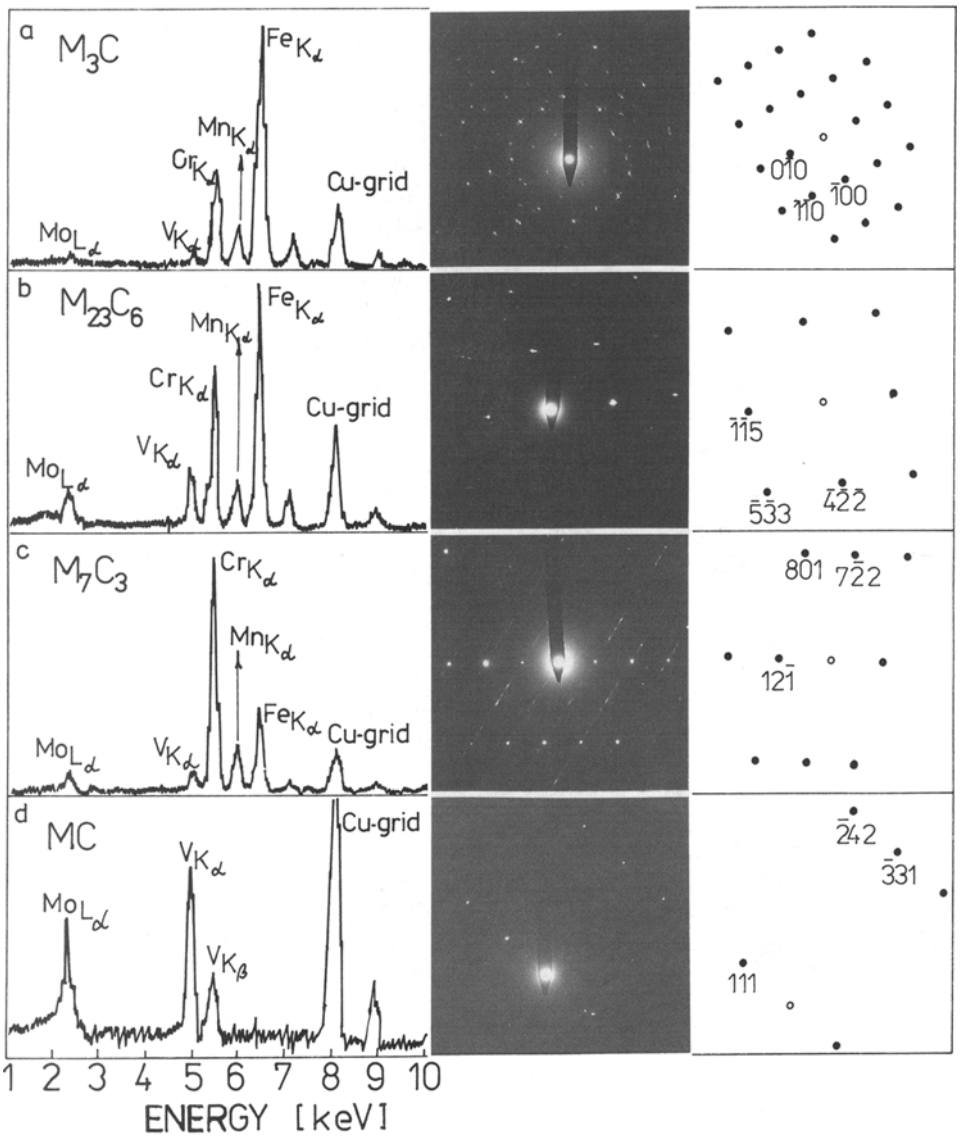

Fig. 5—Characteristic EDX spectra and point electron diffraction patterns used in identification of the carbide phases, TEM: (*a*) M_3C; (*b*) $M_{23}C_6$; (*c*) M_7C_3; and (*d*) MC.

3. M_7C_3 is a stable carbide. Its stability decreases with reduction of the bulk carbon content.
4. M_3C, the least stable carbide, is present only in the microstructure of the low-temperature tempered states, A1 and B1.

Increasing tempering temperature can cause carbide precipitation sequences similar to those caused by the increase of tempering time at the chosen temperature.[18,19] Consequently, the development of the Fe-Cr-rich carbide phases in steels A and B, during tempering at 913 K, can be written as:

$$\varepsilon, Fe_3C \Rightarrow M_3C \Rightarrow M_7C_3 \qquad [1]$$

Carbide $M_{23}C_6$ usually does not belong to the equilibrium phases in Cr-Mo-V steels with bulk Cr content lower than 3 wt pct.[6] Nevertheless, the particles of $M_{23}C_6$ were observed in microstructures of such steels. Senior, in his review paper,[20] showed the scheme of carbide phases precipitation in 1Cr-Mo-V steel, during aging up to 370,800 ks at 723 to 823 K. According to this scheme, $M_{23}C_6$ carbide is replaced by M_7C_3 carbide. Smith[11] has also found the carbide $M_{23}C_6$ in Cr-Mo-V steels with 0.2C, 0.5Mo, <1.5Cr, and <0.4V (wt pct), after aging 7,200 ks at 973 K (Figure 1). He explained this as a result of the stabilizing influence of Mo on the carbide $M_{23}C_6$ in steels with lower Cr-content. According to Smith[11] and Senior,[20] the optimum conditions for precipitation of metastable $M_{23}C_6$ carbide are also at lower Cr and higher Mo content in ferritic matrix. These conditions could be performed during tempering of steels A and B at 823 K. Carbides M_3C and M_7C_3 are Mo-poor, and fine, Mo-rich, MC carbide particles take only a slight volume fraction. Therefore, the Mo content in ferritic matrix is relatively high, and in the areas with reduced Cr-content (*e.g.*, around M_7C_3 particles), it can lead to the formation of individual $M_{23}C_6$ particles. Better diffusivity of elements at higher tempering temperatures and maintenance of higher Cr-content in the

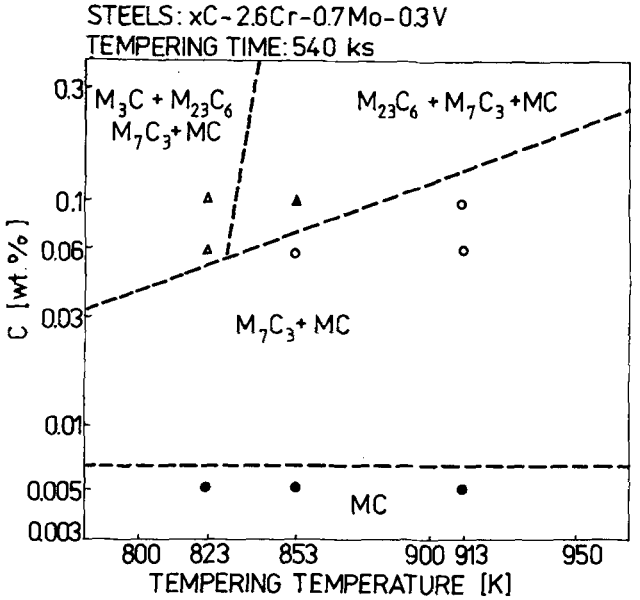

Fig. 6—Constitution diagram of the carbide phases for XC-2.6Cr-0.7Mo-0.3V steels.

matrix, due to lower bulk C-content, can prevent precipitation of this carbide in the states B2, A3, and B3. The carbide $M_{23}C_6$ in steels A and B cannot be considered a stable or equilibrium carbide. The rare presence of its particles in the microstructures of both steels confirms that its precipitation is connected with special conditions in some localities of the matrix.

The particles of Fe_3C carbide present in the microstructure of the quenched state C0, probably lose their stability during the first stage of tempering. Simultaneously, the precipitation of MC carbide starts. For steel C, the following carbide reaction during tempering can be proposed:

$$Fe_3C \Rightarrow MC \qquad [2]$$

Density of particles after 540 ks tempering is higher in state of C2 than in state C1 (Figures 7(g) and (h)). This confirms that the temperature 853 K lies in the interval of the intensive MC precipitation[21] but temperature 823 K does not.

B. *Chemical Composition of Carbides*

From the chemical composition point of view, on the basis of statistical treatment of EDX spectra, the M_3C,

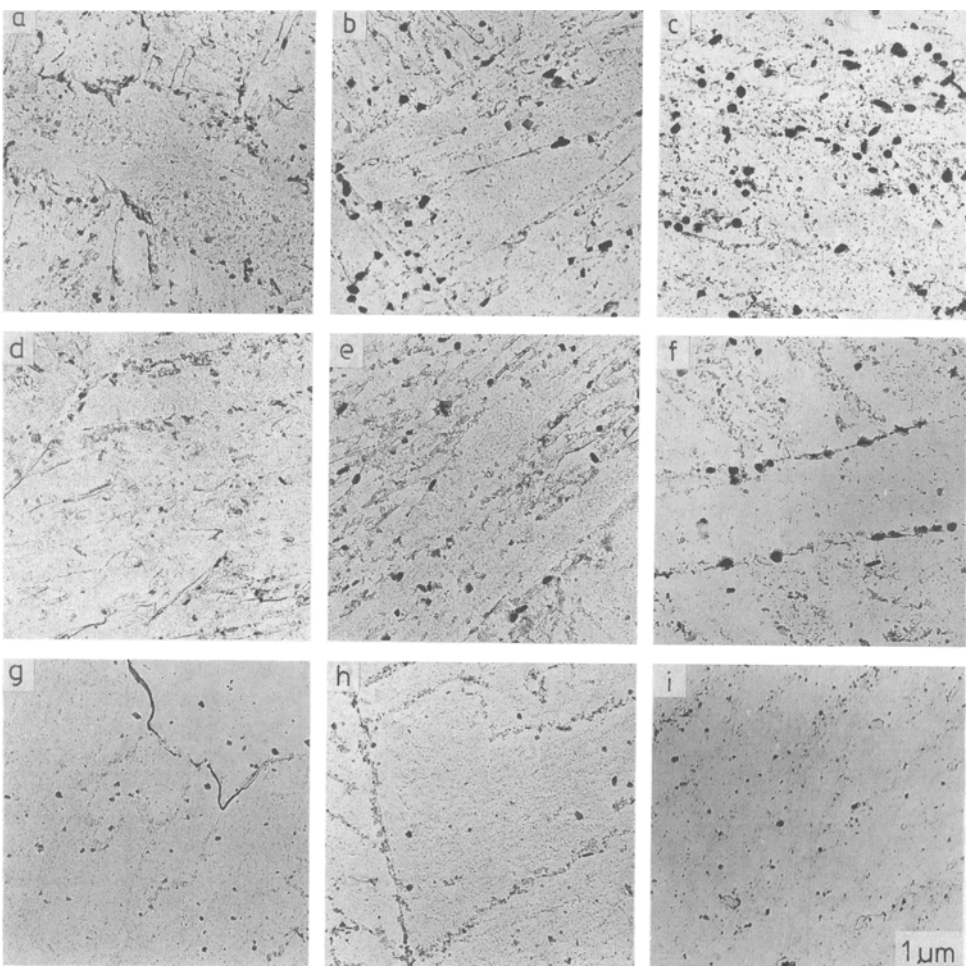

Fig. 7—Carbide particles morphology in the tempered states, TEM, extraction replicas: (*a*) A1; (*b*) A2; (*c*) A3; (*d*) B1; (*e*) B2; (*f*) B3; (*g*) C1; (*h*) C2; and (*i*) C3.

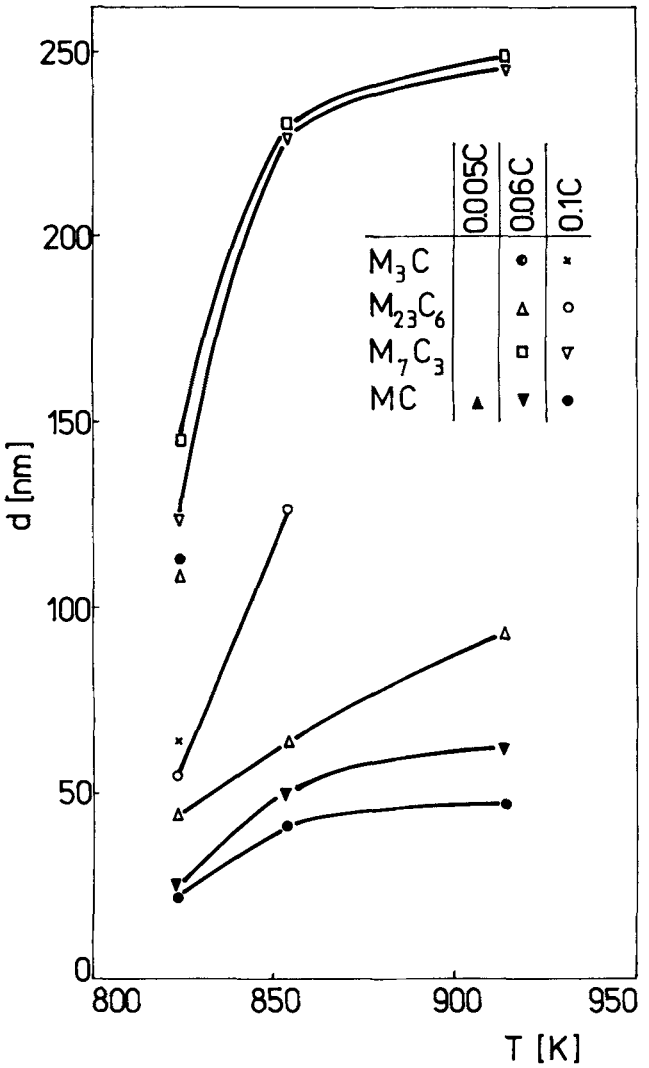

Fig. 8 — Dependence of average sizes of the carbide particles on tempering temperature and bulk C content.

$M_{23}C_6$, and M_7C_3 carbides in steels A and B can be defined as follows:

(a) M_3C is the Fe-rich carbide. The content of Fe is 2.5 times higher than that of Cr. The presence of minor elements Mo, V, and Mn is neglected.
(b) M_7C_3 is the Cr-rich carbide. The Cr content is 2.5 times higher than the Fe content. The presence of minor elements is neglected.
(c) $M_{23}C_6$ is the Fe-Cr-rich carbide. The contents of Fe and Cr are approximately equal; the content of minor elements is slightly increased.

There are differences between the chemical composition of these carbides and the chemical composition of identical carbides in other steels. For instance, Shaw[18] observed the Fe-Cr-rich M_7C_3 carbide in Cr-Mo steels (Figure 2). Elrakayby and Mills[16] found the majority of Cr in the $M_{23}C_6$ carbide in the high-speed 1.1C-4.0Cr-1.5W-9.5Mo-1.1V-8.2Co (wt pct) steel. The results of Stevens and Flewitt[4] and Pilling and Ridley[3] for 2.25Cr-1Mo steel are identical to the results in the present study. Therefore, the characteristic EDX spectra of the Fe-Cr carbides can be spoken about only in relation to the chemical composition of a particular steel or group of steels.

The comparison of the chemical composition of the carbide phases shown in Figure 9 with those studied by Petri *et al.*[22] shows that the next important factor influencing carbide chemical composition is heat treatment. Petri studied the steels 0.11C-2.93Cr-0.54Mo-0.01V and 0.10C-3.95Cr-0.49Mo-0.01V (wt pct) (which have similar chemical composition to steels A and B). After slowly cooling the steels from an austenitization temperature of 773 K, the carbides $M_{23}C_6$ and M_7C_3, with 73 wt pct Cr, 23 wt pct Fe and 20 wt pct Cr, 80 wt pct Fe, respectively, were identified in the steels.

The carbide MC belongs to the carbides with high flexibility of chemical composition.[19] Its constant

Table V. Average Chemical Composition of the Carbides (in Atomic Percent)

Carbide	State	Cr	Mo	V	Fe	Mn	Fe/Cr	V/Mo
M_3C	A1	21	1	4	69	5	3.28	
	B1	32	5	7	51	5	1.59	
$M_{23}C_6$	A1	43	10	3	40	4	0.93	
	A2	36	10	7	42	5	1.17	
	B1	39	10	6	40	5	1.03	
M_7C_3	A1	63	2	5	26	4	0.41	
	A2	60	4	6	25	5	0.42	
	A3	64	4	5	23	4	0.36	
	B1	63	6	6	20	5	0.32	
	B2	63	5	6	22	4	0.35	
	B3	63	4	5	24	4	0.38	
MC	A1		38	62				1.63
	A2		37	63				1.70
	A3		33	67				2.03
	B1		38	62				1.63
	B2		33	67				2.03
	B3		33	67				2.03
	C1		24	76				3.17
	C2		20	80				4.00
	C3		13	87				6.69

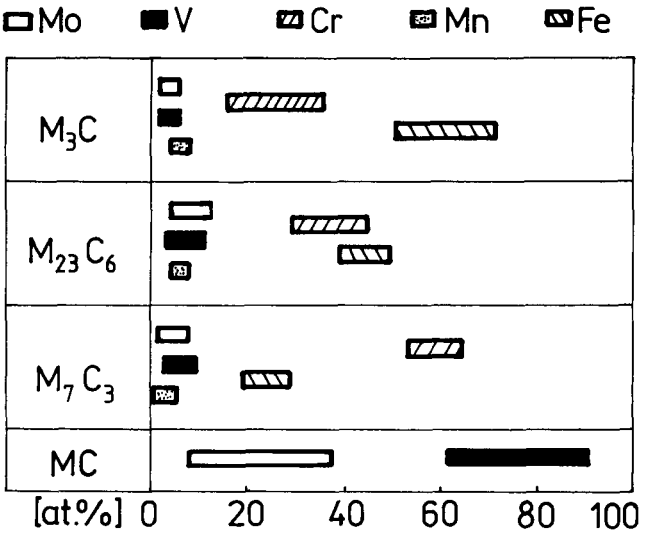

Fig. 9—Chemical composition ranges of the M for M_3C, $M_{23}C_6$, M_7C_3, and MC carbides in 2.6Cr-0.7Mo-0.3V steels.

V/Mo values in the experimental steels A and B confirms that the steels are near the equilibrium state after 540 ks tempering (Table V). This can be explained by relatively low bulk C content in these steels.[1,3] The lack of carbon in a ferrite of steel C encourages its predominant bonding with the strongest carbide-forming element—V. The other alloying elements, including Mo, mostly remain in solid solution.

C. *Morphology and Size of Carbide Particles*

Small ε and Fe_3C carbide particles have plate morphology, the particles of M_3C, $M_{23}C_6$, and M_7C_3 carbides have elongated or equiaxed morphology, and the particles of MC carbide are predominantly equiaxed.

The comparison of the average size and phase stability of the M_3C and M_7C_3 particles shows that the carbide M_7C_3 is larger and also more stable. The particles of M_7C_3 carbide change their size more extremely in the temperature range from 823 to 853 K than from 853 to 913 K. At temperatures above 853 K, the M_3C carbide does not occur (Table IV). It is probable that the loss of M_3C carbide stability at temperatures above 823 K activates the growth of M_7C_3 carbide particles.

D. *Review of Results*

The experimental results given in Figure 6 have been compared with data by Smith.[11] Smith's constitution diagrams show the influence of Cr and V bulk contents on the carbide phase stability in 0.2C-qMo-Cr-V steels, where q = 0.5, 1.0, and 2.0 wt pct, after tempering for 7,200 ks at 973 K. The increase of Mo content from 0.5 to 1.0 wt pct leads to the following changes in the constitution diagram in Figure 1:

(a) the shift of the $M_{23}C_6$ carbide metastable existence line to higher Cr and V concentrations,
(b) the reduction of two-phase area, M_7C_3 + MC, resulted in the enlargement of one-phase M_3C, $M_{23}C_6$, M_7C_3, and MC areas.

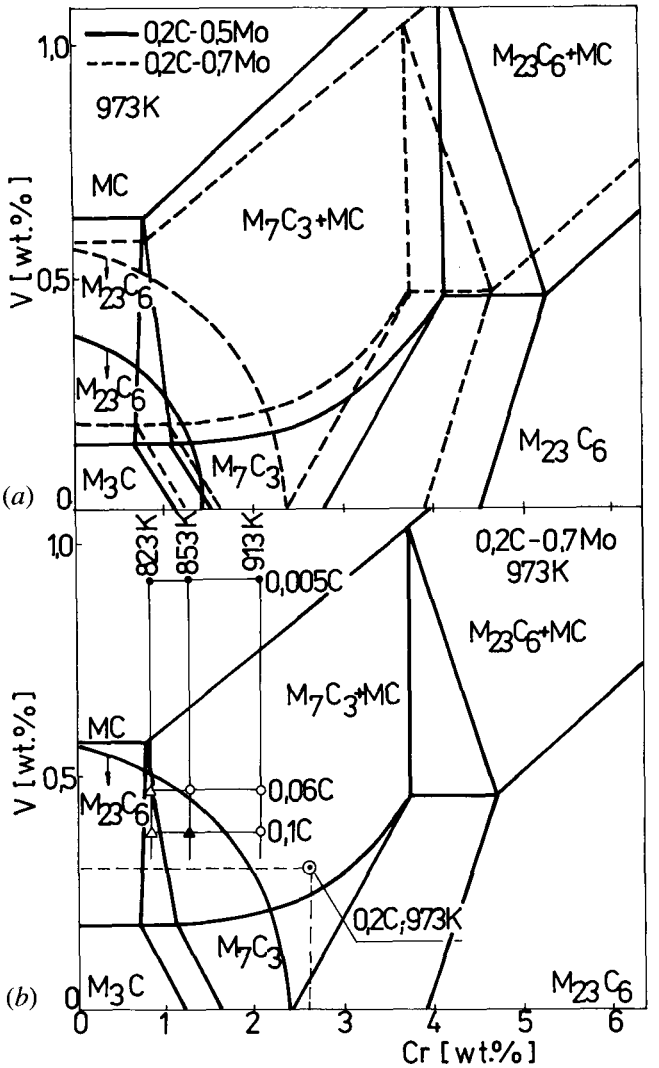

Fig. 10—Constitution diagrams for 0.2C-yCr-qMo-zV steels at 973 K: (*a*) modification of the diagram of the 0.2C-0.5Mo-yCr-zV steels (solid lines) to the diagram for the 0.2C-0.7Mo-yCr-zV (dashed lines) steel;[11] and (*b*) influence of the bulk carbon content and tempering temperature on stability of the carbide phases in the 540 ks tempered xC-2.6Cr-0.7Mo-0.3V steels (the base diagram is for 0.2C-0.7Mo-yCr-zV steel at 973 K).

The constitution diagram for q = 0.7 wt pct Mo, rearranged from the diagram for q = 0.5 wt pct Mo (Figure 10(a)), is shown in Figure 10(b). The dark point in the circle in Figure 10(b) represents 0.2C-2.6Cr-0.7Mo-0.3V steel. It is evident from the position of this point that the equilibrium state of the steel at 973 K contains M_7C_3 and MC carbides. The experimental points from Figure 6 are simultaneously plotted to the appropriate areas in Figure 10(b). In comparison with the dark point in the circle, they have different carbon content and T_T. The analysis of Figures 6 and 10(b) indicates the following information for the xC-2.6Cr-0.7Mo-0.3V (x < 0.2 wt pct) steels:

(a) The decrease of tempering temperature has the same influence on the stability of carbide phases as the decrease of bulk Cr content at the unchanged V, Mo, and C bulk contents.
(b) The decrease of bulk carbon content has the same

influence on the stability of carbide phases as the increase of bulk V content at the unchanged Cr, Mo, C bulk contents and tempering temperature.
(c) After 540 ks tempering at $T_T < 823$ K, three other combinations of phase composition are possible: M_3C + MC, M_3C + $M_{23}C_6$ + MC, and M_3C + M_7C_3 + MC.

V. CONCLUSIONS

The results of the carbide particles investigation in the quenched and 540 ks tempered states of 2.6Cr-0.7Mo-0.3V steel with various carbon content can be summarized as follows:

1. In the ferritic-carbidic microstructures of the tempered states, four types of carbides were identified: M_3C (Fe-rich), $M_{23}C_6$ (Fe-Cr-rich), M_7C_3 (Cr-rich), and MC (V-Mo-rich). In microstructures of the quenched states, only ε and M_3C carbides were present.
2. The changes of the bulk carbon content have a minimal influence on the characteristic EDX spectra of the identified carbides. The influence of the tempering temperature is more telling only in the case of the M_3C and MC carbides.
3. From the phase stability point of view, the most stable are carbides MC and M_7C_3.
4. The decrease of tempering temperature has the same influence on the carbide phases stability as the decrease of bulk Cr content at the unchanged V, Mo, and C bulk contents.
5. The decrease of bulk carbon content has the same influence on the carbide phases stability as the increase of bulk V content at the unchanged Cr, Mo, and C bulk contents, and tempering temperature.

REFERENCES

1. K. Kuo: *J. Iron Steel Inst.*, 1953, vol. 173, pp. 363-75.
2. K.H. Kuo and C.L. Jia: *Acta Metall.*, 1985, vol. 33, pp. 991-96.
3. J. Pilling and N. Ridley: *Metall. Trans. A*, 1982, vol. 13A, pp. 557-63.
4. R.A. Stevens and P.E.J. Flewitt: *Acta Metall.*, 1986, vol. 34, pp. 849-66.
5. J. Purmensky, V. Foldyna, B. Million, and J. Vrestal: *Kovove. Mater.*, 1980, vol. 18, pp. 171-88.
6. K.W. Andrews, H. Hughes, and D.J. Dyson: *J. Iron Steel Inst.*, 1972, vol. 210, pp. 337-50.
7. J. Yu and C.J. McMahon, Jr.: *Metall. Trans. A*, 1980, vol. 11A, pp. 277-89.
8. R.G. Baker and J. Nutting: *J. Iron Steel Inst.*, 1959, vol. 192, pp. 257-68.
9. T. George, E.R. Parker, and O.R. Ritchie: *Mater. Sci. Technol.*, 1985, vol. 1, pp. 198-208.
10. J. Cadek, O. Dupal, and R. Freiwillig: *Hut. Listy*, 1962, vol. 17, pp. 573-80.
11. R. Smith: ISI Special Report, 1959, vol. 64, pp. 307-11.
12. S.W.K. Shaw and A.G. Quarrell: *J. Iron Steel Inst.*, 1957, vol. 185, pp. 10-22.
13. J.H. Woodhead and A.G. Quarrell: *J. Iron Steel Inst.*, 1965, vol. 203, pp. 605-20.
14. J. Janovec: *Neue Huette*, 1992, vol. 37, pp. 281-86.
15. J. Janovec, A. Güth, A. Vyrostkova, and B. Stefan: *Neue Huette*, 1989, vol. 34, pp. 91-96.
16. A.M. Elrakayby and B. Mills: *J. Mater. Sci. Lett.*, 1986, vol. 5, pp. 332-34.
17. H. Zuo and J.S. Kirkaldy: *Metall. Trans. A*, 1991, vol. 22A, pp. 1511-24.
18. B.J. Shaw: *Research on chrome-moly steels*, R.A. Swift, ed., ASME, New York, NY, 1984, vol. MPC-21, pp. 117-26.
19. J. Janovec, A. Vyrostkova, and A. Holy: *J. Mater. Sci.*, 1992, vol. 27, pp. 6564-72.
20. B.A. Senior: *Mater. Sci. Eng.*, 1988, vol. A103, pp. 263-71.
21. I. Hrivnak: *Weldability of steels*, ALFA, Bratislava, 1979, pp. 127-38.
22. R. Petri, E. Schnabel, and P. Schwaab: *Arch. Eisenhüttenwes.*, 1981, vol. 52, pp. 71-76.